Observation of quantum interference between dressed states in an electromagnetically induced transparency

Yong-qing Li and Min Xiao
Department of Physics, University of Arkansas, Fayetteville, Arkansas 72701
(Received 31 January 1995)

We report on an experimental observation of quantum interference between two dressed states created by a coherent pumping laser in an electromagnetically induced transparency. In a Λ-type three-level atomic system in rubidium vapor, we reduce the Rabi frequency of the pumping laser in one arm down below the spontaneous decay rate of the common excited state and still observe a narrow dip with subnatural linewidth in the absorption curve of a probe beam in another arm. This clearly demonstrates that the absorption reduction at the low pumping intensity is mainly due to the interference between the two dressed states, not due to the ac–Stark-shift effect.

PACS number(s): 42.50.Rh, 42.50.Md, 32.80.Wr, 42.65.Ky

Recently, Imamoğlu and Harris have shown that destructive interference between dressed lifetime-broadened states created by an additional (pumping) electromagnetic field produces a zero absorption (dip) in the absorption profile of a weak probe field in a three-level atomic system [1]. This destructive interference between the transition probability amplitudes from the ground state to the excited doublets (dressed states) is a Fano-type interference and plays an important role in lasing without inversion [2,3] and in electromagnetically induced transparency (EIT) [4–7]. However, in all the previous EIT experiments [4–7], the pumping Rabi frequency is relatively large compared to the lifetime-broadened decay rate of the dressed states and, therefore, the reduction in the absorption at resonance is the result of a combination of the ac-Stark shift and the interference of dressed states [4]. In this paper, we report an experiment done in a Doppler-broadened rubidium vapor cell with the pumping Rabi frequency well below the decay rate of the dressed states. A narrow dip with subnatural linewidth in the center of the absorption profile was observed. Due to the fact that the ac-Stark shift has a negligible contribution to the dip in the absorption profile for the pumping Rabi frequency used in our experiment, the observed reduction in the absorption profile is direct evidence of interference between the dressed lifetime-broadened states.

Note in Fig. 1, when a resonant pumping field (with Rabi frequency Ω_2) is applied to the transition $|3\rangle-|2\rangle$, the common excited state $|2\rangle$ can be viewed as two dressed states ($|2d\rangle$ and $|3d\rangle$), separated by pumping Rabi frequency Ω_2 through the ac-Stark splitting or Autler-Townes effect. When a weak probe beam (with Rabi frequency Ω_1) is tuned to the transition from state $|1\rangle$ to the middle of the two dressed states $|2d\rangle$ and $|3d\rangle$ (which is the transition $|1\rangle-|2\rangle$ in the bare-state picture), two effects will contribute to the absorption reduction of the probe field. One is the ac-Stark shift (states $|3d\rangle$ and $|2d\rangle$ are shifted by $\pm\Omega_2/2$ from the probe resonance, respectively) and the other is the interference between the two transition paths of $|1\rangle-|2d\rangle$ and $|1\rangle-|3d\rangle$. Since these two quantum-mechanical paths couple to the same final level $|2\rangle$ by the coherent pumping field, Fano-type destructive interference [8] occurs and leads to zero absorption. Following Refs. [1] and [2], the equations for the time-varying amplitudes of ground level $|1\rangle$ (C_1) and of upper dressed levels $|2d\rangle$(C_{2d}) and $|3d\rangle$ (C_{3d}) can be expressed as

$$\frac{\partial C_1}{\partial t}=-\frac{\Gamma_3}{2}C_1-i\frac{\Omega_1^*}{2}(C_{2d}\cos\theta+C_{3d}\sin\theta)\ ,$$
$$\frac{\partial C_{2d}}{\partial t}=\left[-\frac{\Gamma_{2d}}{2}+i\Delta_{2d}\right]C_{2d}-i\frac{\Omega_1}{2}C_1\cos\theta+\kappa_{23}C_{3d}\ , \quad (1)$$
$$\frac{\partial C_{3d}}{\partial t}=\left[-\frac{\Gamma_{3d}}{2}+i\Delta_{3d}\right]C_{3d}-i\frac{\Omega_1}{2}C_1\sin\theta+\kappa_{23}C_{2d}\ .$$

The quantities in these equations and the relations between bare states ($|2\rangle$ and $|3\rangle$) and dressed states ($|2d\rangle$ and $|3d\rangle$) are given by

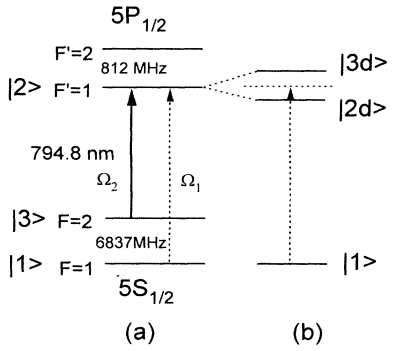

FIG. 1. Relevant energy diagram of the $D1$ line of the Rb^{87} atom. (a) Bare-state picture; (b) dressed-state picture. The pumping laser is represented by the solid line and probe laser is represented by the dashed line.

$$\Delta_{2d}=\Delta_1-\Delta_2/2+R/2\ ,\quad \Delta_{3d}=\Delta_1-\Delta_2/2-R/2\ ,$$
$$\Gamma_{2d}=\Gamma\cos^2\theta+\Gamma_3\sin^2\theta\ ,\quad \Gamma_{3d}=\Gamma\sin^2\theta+\Gamma_3\cos^2\theta\ ,$$
$$\kappa_{23}=-\frac{\Gamma-\Gamma_3}{4}\sin 2\theta\ ,\quad \Gamma=\Gamma_1+\Gamma_2\ ,\quad R=\sqrt{\Delta_2^2+\Omega_2^2}\ , \tag{2}$$
$$|2d\rangle=\cos\theta|2\rangle-\sin\theta|3\rangle\ ,\quad |3d\rangle=\sin\theta|2\rangle+\cos\theta|3\rangle\ ,$$

where $\tan 2\theta=\Omega_2/\Delta_2$; Γ_1 and Γ_2 are the decay rates of level $|2\rangle$ to level $|1\rangle$ and level $|3\rangle$, respectively; Γ_3 is the nonradiative transition rate from level $|3\rangle$ to level $|1\rangle$ and from level $|1\rangle$ to $|3\rangle$; Δ_1 and Δ_2 are detunings of the probe field and pumping field from atomic resonances, respectively; and Ω_1 and Ω_2 are the respective Rabi frequencies ($\mu E/\hbar$) of the probe field and pumping field.

The terms proportional to Δ_{2d} and Δ_{3d} in Eqs. (1) represent ac-Stark shifts of the dressed states $|2d\rangle$ and $|3d\rangle$ from the bare level $|2\rangle$. The cross terms (proportional to κ_{23}) in Eqs. (1) indicate that, as level $|2d\rangle$ decays, it drives level $|3d\rangle$ to decay as well and vice versa, since both levels couple to the same bare level $|2\rangle$ by a coherent pumping field. As pointed out by Harris [2], these cross terms are essential in creating destructive interference of transition-probability amplitudes between transitions $|1\rangle-|2d\rangle$ and $|1\rangle-|3d\rangle$.

A detailed procedure of solving Eqs. (1) was given in Refs. [1] and [2]. Here we only give the result for a special case of $\Gamma_3=0$ and $\Delta_2=0$. In such a case, the lifetime-broadened decay rates of the dressed states $|2d\rangle$ and $|3d\rangle$ are $\Gamma_{2d}=\Gamma_{3d}=\Gamma/2$ and the detuning shifts are $\Delta_{2d}=\Delta_1+\Omega_2/2$ and $\Delta_{3d}=\Delta_1-\Omega_2/2$. The transition rate $W_{ab}=-(\partial/\partial t)|C_1(t)|^2$ for absorption of the probe field is obtained from Eqs. (1) to be [2]

$$W_{ab}=\frac{\Omega_1^2}{2}\mathrm{Re}\left\{\frac{-i\Delta_1+(\kappa_{23}+\Gamma/4)}{[\Gamma/4-i(\Delta_1+\Omega_2/2)][\Gamma/4-i(\Delta_1-\Omega_2/2)]-\kappa_{23}^2}\right\}=\frac{\Omega_1^2\Gamma\Delta_1^2}{\Delta_1^2\Gamma^2+4(\Delta_1^2-\Omega_2^2/4)^2}\ . \tag{3}$$

Note that zero absorption appears at the center ($\Delta_1=0$) of probed absorption profile Eq. (3). To separate the effect of the ac-Stark shifts from the quantum interference of dressed states on the absorption profile, we remove the interference terms (proportional to κ_{23}) in Eqs. (1). The resulting equations describe the absorption of an atom from level $|1\rangle$ to two independent levels (with an identical decay rate of $\Gamma/2$) separated by $\pm\Omega_2/2$ from the probe transition frequency. The transition rate W'_{ab} for absorption is then given by

$$W'_{ab}=\frac{\Omega_1^2\Gamma}{16}\left[\frac{1}{\Gamma^2/16+(\Delta_1+\Omega_2/2)^2}+\frac{1}{\Gamma^2/16+(\Delta_1-\Omega_2/2)^2}\right], \tag{4}$$

which is the superposition of two Lorentz absorption profiles. Figure 2 plots the transition rates W'_{ab} and W_{ab} for different pumping Rabi frequencies, respectively. It can be seen from Fig. 2 that, as Ω_2 becomes smaller than the dressed-state linewidth ($\Gamma/2$), ac-Stark shifts make a negligible contribution to the dip of the absorption profile. Especially, as $\Omega_2\leq 0.3\Gamma$, there is no dip in the absorption profile W'_{ab} due to the ac-Stark shifts alone. However, due to the destructive interference of dressed states, the zero absorption dip still remains at the center of the absorption profile W_{ab}. From this observation, one can conclude that, when the pumping Rabi frequency is smaller than the linewidth of the dressed states, the absorption reduction at the center frequency of the profile is dominated by the effect of quantum interference of the transition probability amplitudes between dressed states. The curves in Fig. 2 calculated from Eqs. (3) and (4) do not include Doppler-broadening effects.

To directly observe the destructive quantum interference of dressed states in a Doppler-broadened vapor system, we have to take into account the effects of the nonradiative decay rate Γ_3 and Doppler-broadening effect. These effects severely degrade the degree of destructive interference, especially at low-pumping Rabi frequencies. With Doppler-broadening and nonradiative decay rate Γ_3 being included, the complex susceptibility of the probe

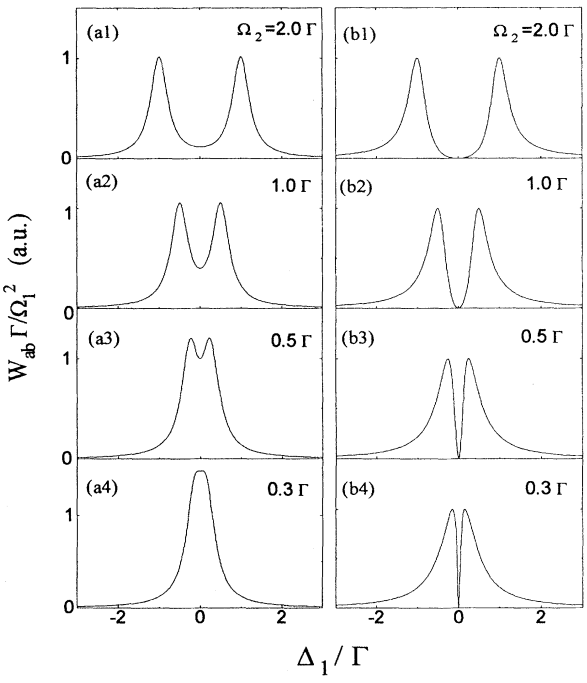

FIG. 2. Absorption rates W'_{ab} (ac-Stark shift only, left column) and W_{ab} (ac-Stark shift plus quantum interference, right column) vs probe frequency with $\Gamma_3=0$ and no Doppler-broadening effect. (a1) and (b1) $\Omega_2=2.0\Gamma$, (a2) and (b2) $\Omega_2=1.0\Gamma$, (a3) and (b3) $\Omega_2=0.5\Gamma$, (a4) and (b4) $\Omega_2=0.3\Gamma$.

transition is given by [6,7]

$$\chi=\frac{ic\mu_{21}^2 N_0\sqrt{\pi}}{\hbar\omega_1}e^{z^2}[1-\mathrm{erf}(z)]\ , \tag{5}$$

with the argument

$$z=\frac{c}{\omega_1 u}\left[\frac{\Gamma+\Gamma_3}{2}-i\Delta_1+\frac{\Omega_2^2/4}{\Gamma_3-i(\Delta_1-\Delta_2)}\right]\ , \tag{6}$$

where $\mathrm{erf}(z)$ is the error function with complex argument z, ω_1 the probe frequency, N_0 the density of atoms, and $u/\sqrt{2}$ the root-mean-square atomic velocity. The imaginary part $\mathrm{Im}(\chi)$ is proportional to the absorption coefficient of the atomic medium. In Eq. (5), we have assumed that the pumping beam and probe beam pass through the Doppler-broadened medium in the same direction.

From Eq. (5), it is easily shown that the condition for significant absorption reduction is given by $\Omega_2\sim\sqrt{\Delta\omega_D\Gamma_3}$, where $\Delta\omega_D=2\sqrt{\ln 2}\omega_p u/c$ is the Doppler linewidth [6]. In a rubidium vapor cell near room temperature, $\Delta\omega_D\sim 540$ MHz, $\Gamma_3\sim 10$ kHz, this condition reaches $\Omega_2\sim 2.3$ MHz, which is about 0.38Γ ($\Gamma=6.0$ MHz for the $D1$ line of Rb^{87} atoms). Although the condition of $\Omega_2<\Gamma/2$ for the disappearance of the effect due to the ac-Stark shift will loosen in a Doppler-broadened medium, we will keep it as an ultimate test for the demonstration of quantum interference in our experiment.

The experiment was done in a three-level Λ-type system in Rb^{87} atoms. Considering the $D1$ line at 794.8 nm (the transition from $5S_{1/2}$ to $5P_{1/2}$) in Fig. 1, the hyperfine levels $F=1$ and $F=2$ of $5S_{1/2}$ serve as ground states $|1\rangle$ and $|3\rangle$. The hyperfine level $F'=1$ of $5P_{1/2}$ serves as the common excited state. Another hyperfine level $F'=2$ is about 812 MHz from the $F'=1$ level and is outside the Doppler linewidth $\Delta\omega_D$. Therefore, its effect can be neglected. This is an ideal closed three-level Λ-type system to study EIT. The coherent pumping field with Rabi frequency Ω_2 and detuning Δ_2 is tuned to the transition $(F=2)$-$(F'=1)$ (solid line), and the weak probe field with Rabi frequency Ω_1 is scanned across the transition $(F=1)$-$(F'=1)$ (dotted line). The spontaneous decay rate Γ_2 from level $|2\rangle$ to level $|3\rangle$ is about five times that of the spontaneous decay rate Γ_1 from level $|2\rangle$ to level $|1\rangle$, and the total decay rate Γ of the excited level $|2\rangle$ is about 6.0 MHz.

The experimental arrangement is given in Fig. 3. The Doppler-free configuration for the atomic coherence effect (the pumping beam and probe beam propagate colinearly through the atomic vapor cell) in a Λ-type system is used [7]. This configuration can reduce the requirement for the pumping intensity to create effective atomic coherence, since the atomic coherence ρ_{31} depends on the two-phonon resonance $\omega_1-\omega_{21}=\omega_2-\omega_{23}$, where ω_1 and ω_2 are the frequencies of probe field and pumping field, respectively, and ω_{21} and ω_{23} are the resonant frequencies of transitions from level $|2\rangle$ to level $|1\rangle$ and from level $|2\rangle$ to level $|3\rangle$, respectively. For atoms with velocity v, the Doppler shift for the probe beam is $\omega_1 v/c$, and for the pumping beam is $\omega_2 v/c$, which are about the same for $\omega_1\approx\omega_2$ and can be canceled in two-photon resonance condition. So all the atoms with different velocities satisfy the condition of two-photon resonance, which produces effective atomic coherence ρ_{31} and contributes to the transparency of the probe field. The 45-mm-long rubidium vapor cell is kept at a temperature of 53.5°C, which gives the atomic density of $N\approx 2\times 10^{11}$ atoms/cm^3. The maximum absorption of the probe field at the transition $5S_{1/2}$, $F=1$-$5P_{1/2}$, $F'=1$ is about 30% without the pumping field. The cell is shielded with μ metal from the surrounding magnetic field to avoid the magnetic-field splitting of the sublevels. A diode laser DL1 serves as a probe laser, and a diode laser DL2 as a pumping laser. Both diode lasers are frequency stabilized to give a frequency slow jitters below 0.5 MHz during our sampling time ($\sim$10 ms). To get a good spatial match, the pumping beam and probe beam are orthogonally polarized and two apertures are used. An aperture (AP1) of 1.2 mm diameter in front of the vapor cell is intended to make the same beam size of the pumping beam and probe beam. At low atomic density, the nonradiative relaxation constant Γ_3 is determined by the time-of-flight of atoms through the laser beam (the diameter of AP1), which is about $\Gamma_3\sim 40$ kHz. An aperture (AP2) of 0.5-mm diameter in front of the detector is used to measure the central part of the probe beam only. A polarizer is used in front of the detector to eliminate scattered pumping light from cell surfaces. The probe power is typically 0.1 μW, corresponding to an intensity of 10 μW/cm^2, which is well below the saturation intensity of $I_{\mathrm{sat}}\approx 1.67$ mW/cm^2 for the maximum transition [9].

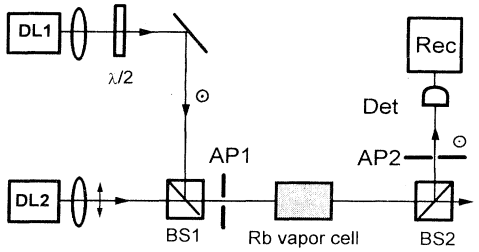

FIG. 3. Experimental arrangement DL1, diode laser for probe beam; DL2, diode laser for pumping beam; BS1 and BS2, polarization cube beam splitter; AP1 and AP2, apertures; Det, photodetector; Rec, recorder; $\lambda/2$, half-wave plate.

To directly observe the Fano-type interference effect, we reduce the pumping power to near saturation intensity. In this case, the input pumping power decreases significantly as it propagates through the cell due to absorption in the pumping transition. Thus, we need to measure both the input and output powers of the pumping beam. We will only give the input pumping intensity and estimate the mean Rabi-frequency for simplicity. Measurements of the absorption at transition $5S_{1/2}$, $F=1$-$5P_{1/2}$, $F'=1$ for different pumping intensities are given in Fig. 4. Figure 4(a) is with no pumping beam ($\Omega_2=0$) and is used as a reference. Figure 4(b) is for the input pumping power of $P_{\mathrm{in}}=267$ μW with estimated mean Rabi frequency $\Omega_2\sim 2.0\Gamma$ [9]. A 55.2% absorption

reduction at the center frequency with 7.5 MHz full width at half maximum (FWHM) linewidth of the dip is observed. Figure 4(c) is for an input pumping power of 73 μW with mean Rabi frequency $\Omega_2 \sim 1.1\Gamma$. A 35.7% absorption reduction with 3.9 MHz FWHM of the dip is observed. When the pumping power is reduced further to 8.3 μW, a significant absorption reduction (about 15.5%) still survives, as shown in Fig. 4(d). In this case, the average pumping Rabi frequency Ω_2 is only about 0.3Γ, which is much smaller than the natural linewidth of the excited-state decay rate Γ. The linewidth of the dip is about 1.4 MHz ($\sim 0.23\Gamma$), which is also smaller than the natural linewidth Γ. Although the reduction in absorption is small in the last case, it cannot be explained by the conventional Rabi-splitting or the ac–Stark-shift effect, as discussed above. It is direct evidence of quantum interference between dressed states.

The linewidth of the narrow dip is limited by the pumping Rabi frequency Ω_2 and the ground-state decay rate Γ_3. The observed linewidth of the dip is found to be linearly proportional to the pumping Rabi frequency at low pumping power, since $\Gamma_3 \ll \Omega_2$ in our case. The reduction in absorption at low pumping power is currently limited by the laser linewidths (fast fluctuations of laser frequency) of both the pumping laser and the probe laser. In our case, the beat frequency of the two lasers is found to have a 4.7-MHz FWHM linewidth. With narrower linewidth lasers, we expect to observe a larger reduction in probe absorption for an even smaller pumping intensity.

In summary, the Fano-type interference effect is directly observed in a closed three-level Λ-type atomic system in a rubidium vapor cell. The size of the effect is currently limited by the laser linewidths of both the pumping laser and the probe laser. The Doppler broadening of the atoms in the cell also degrades the interference effect. However, the direct observation of this Fano-type interference effect is very important in proving the existence of a quantum interference effect in EIT experiments. This closed three-level Λ-type system is ideal for studying quantum phase correlation and squeezing effects, as proposed recently [10,11].

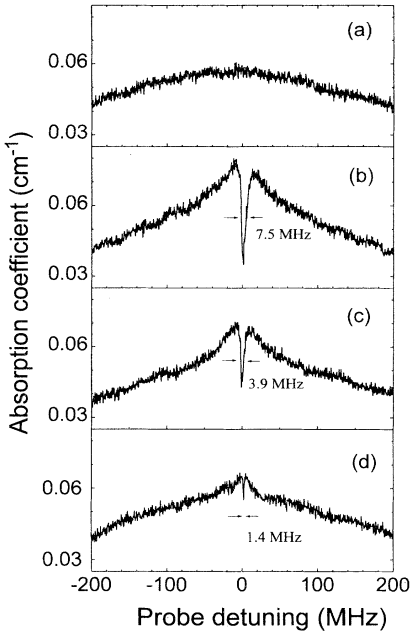

FIG. 4. Absorption coefficient vs probe detuning for transition $(F=1)$–$(F'=1)$ for (a) no pumping power ($\Omega_2=0$), (b) Rabi frequency $\Omega_2 \sim 2.0\Gamma$, (c) $\Omega_2 \sim 1.1\Gamma$, and (d) $\Omega_2 \sim 0.3\Gamma$.

We acknowledge financial support from the Office of Naval Research and the National Science Foundation through Grant Nos. PHY9221718 and PHY9457905 (NYI Program).

[1] A. Imamoğlu and S. E. Harris, Opt. Lett. **14**, 1344 (1989).
[2] S. E. Harris, Phys. Rev. Lett. **62**, 1033 (1989).
[3] E. Fry *et al.*, Phys. Rev. Lett. **70**, 3235 (1993); W. E. van der Veer *et al.*, *ibid.* **70**, 3243 (1993); A. Nottelmann *et al.*, *ibid.* **70**, 1783 (1993).
[4] K.-J. Boller, A. Imamoğlu, and S. E. Harris, Phys. Rev. Lett. **66**, 2593 (1991); J. E. Field, K. H. Hahn, and S. E. Harris, *ibid.* **67**, 3062 (1991).
[5] K. Hakuta, L. Marmet, and B. P. Stoicheff, Phys. Rev. Lett. **66**, 596 (1991); G. Z. Zhang, K. Hahuta, and B. P. Stoicheff, *ibid.* **71**, 3099 (1993).
[6] J. Gea-Banacloche, Y. Q. Li, S. Jin, and M. Xiao, Phys. Rev. A **51**, 576 (1995); M. Xiao, Y. Q. Li, S. Jin, and J. Gea-Banacloche, Phys. Rev. Lett. **74**, 666 (1995).
[7] Y. Q. Li and Min Xiao, Phys. Rev. A **51**, R2703 (1995).
[8] U. Fano, Phys. Rev. **124**, 1866 (1961); U. Fano and J. W. Cooper, *ibid.* **137**, 1364 (1965).
[9] The saturation intensity I_0 and pumping Rabi frequency Ω_2 used in our experiment are estimated by $I_0=\pi hc\Gamma/(3\lambda^3)$ and $\Omega_2=\Gamma\sqrt{I/(2I_0)}$, where λ is the wavelength and I is the pumping intensity. It should be noted that this estimation does not include the magnetic hyperfine transitions of the pumping transition. So, our estimated Rabi frequency Ω_2 represents the value for the sublevel transition with the maximum transition rate. The mean value of Ω_2 over different sublevel transitions will be smaller than this value.
[10] K. M. Gheri and D. F. Walls, Phys. Rev. Lett. **68**, 3428 (1992); Phys. Rev. A **46**, R6793 (1992); *ibid.* **49**, 4134 (1994).
[11] M. Fleischhauer, Phys. Rev. Lett. **72**, 989 (1994); G. S. Agarwal, *ibid.* **71**, 1351 (1993).